OXFORD

SOT | Society of Toxicology
www.toxsci.oxfordjournals.org

TOXICOLOGICAL SCIENCES, 168(2), 2019, 460–473

doi: 10.1093/toxsci/kfz016
Advance Access Publication Date: January 14, 2019
Research Article

Bromate-induced Changes in *p21* DNA Methylation and Histone Acetylation in Renal Cells

Ramya T. Kolli,[*,†,1] Travis C. Glenn,[†,‡] Bradley T. Brown,[§] Sukhneeraj P. Kaur,[*] Lillie M. Barnett,[*,†] Lawrence H. Lash,[¶] and Brian S. Cummings[*,†,2]

[*]Department of Pharmaceutical and Biomedical Sciences; [†]Interdisciplinary Toxicology Program; [‡]Environmental Health Science; [§]College of Pharmacy, University of Georgia, Athens, Georgia 30602; and [¶]Department of Pharmacology, Wayne State University, Detroit, Michigan 48201

[1]Present address: National Institute of Environmental Health Sciences, Building 101, 111 TW Alexander Drive, Durham, NC 27709.
[2]To whom correspondence should be addressed at 336 College of Pharmacy South, University of Georgia, Athens, GA 30602. Fax: (706) 542-5358. E-mail: briansc@uga.edu.

ABSTRACT

Bromate (BrO_3^-) is a water disinfection byproduct (DBP) previously shown to induce nephrotoxicity *in vitro* and *in vivo*. We recently showed that inhibitors of DNA methyltransferase 5-aza-2′-deoxycytidine (5-Aza) and histone deacetylase trichostatin A (TSA) increased BrO_3^- nephrotoxicity whereas altering the expression of the cyclin-dependent kinase inhibitor p21. Human embryonic kidney cells (HEK293) and normal rat kidney (NRK) cells were sub-chronically exposed to BrO_3^- or epigenetic inhibitors for 18 days, followed by 9 days of withdrawal. DNA methylation was studied using a modification of bisulfite amplicon sequencing called targeted gene bisulfite sequencing. Basal promoter methylation in the human *p21* promoter region was substantially lower than that of the rat DNA. Furthermore, 5-Aza decreased DNA methylation in HEK293 cells at the sis-inducible element at 3 distinct CpG sites located at 691, 855, and 895 bp upstream of transcription start site (TSS). 5-Aza also decreased methylation at the rat *p21* promoter about 250 bp upstream of the *p21* TSS. In contrast, sub-chronic BrO_3^- exposure failed to alter methylation in human or rat renal cells. BrO_3^- exposure altered histone acetylation in NRK cells at the *p21* TSS, but not in HEK293 cells. Interestingly, changes in DNA methylation induced by 5-Aza persisted after its removal; however, TSA- and BrO_3^--induced histone hyperacetylation returned to basal levels after 3 days of withdrawal. These data demonstrate novel sites within the *p21* gene that are epigenetically regulated and further show that significant differences exist in the epigenetic landscape between rat and human *p21*, especially with regards to toxicant-induced changes in histone acetylation.

Key words: kidney; nephrotoxicity; epigenetics; *p21*; chromatin immunoprecipitation; bromate; DNA methylation; next-generation sequencing.

Ozonation is an extensively used method for disinfection of source water (US-EPA, 1998a). Bromate (BrO_3^-) is a disinfection byproduct (DBP) formed by the reaction of ozone with naturally occurring bromide (Br^-) in water, and BrO_3^- is designated as a probable human carcinogen by the International Agency for Research on Cancer (IARC, 1999). The maximum contaminant level (MCL) for BrO_3^- established by the United States Environmental Protection Agency (US-EPA) is 0.01 ppm (US-EPA, 1998b, 2012), which is usually less than what is formed after ozonation of source waters.

The kidney is a major target organ for BrO_3^--induced toxicity (Kurokawa *et al.*, 1982), and BrO_3^- has been shown to induce renal cell tumors in rats after chronic exposures (Kurokawa *et al.*, 1990). BrO_3^- also induces DNA damage characterized by 8-OHdG (8-hydroxyguanosine) production, which is also a measure of oxidative stress *in vitro* and *in vivo* (Kawanishi and Murata, 2006). We previously reported that BrO_3^- induces a G2/M cell cycle arrest prior to the occurrence of cell death, and increases the expression of stress response kinases and DNA damage response proteins such as p38 and mitogen-activated protein

kinase (Zhang *et al.*, 2010, 2011). We have also demonstrated that BrO_3^- increases the expression of the cyclin-dependent kinase inhibitor p21, both *in vitro* and *in vivo* (Kolisetty, Bull, *et al.*, 2013; Zhang *et al.*, 2010).

p21 regulates cell cycle progression at the G1 and S phase (Gartel and Radhakrishnan, 2005). p21 activation has been shown to be protective against various nephrotoxicants such as cisplatin (di Pietro *et al.*, 2012; Jiang and Dong, 2008; Nowak *et al.*, 2003; Price *et al.*, 2009). Several studies have shown that p21 can be activated by the tumor suppressor p53, and that such activation correlates with cell death (el-Deiry *et al.*, 1994). However, our recent studies demonstrate that exposure of both cells and animals to lower, more environmentally relevant doses of BrO_3^- resulted in p21 activation independently of p53 (Kolisetty, Bull, *et al.*, 2013; Kolisetty, Delker, *et al.*, 2013; Scholpa *et al.*, 2014). Hence, this study was focused on understanding the alternative mechanism mediating how BrO_3^- activates p21 independently of p53.

As aforementioned, we previously demonstrated, using immunoblot analysis, that sub-chronic exposure of renal cells to doses of BrO_3^- as low as 0.01 ppm (MCL) increased p21 protein expression (Scholpa *et al.*, 2014). To our knowledge these were some of the lowest doses ever shown for BrO_3^- to induce molecular changes. This same study also showed that BrO_3^- exposure altered methylation of the coding region of *p21* in correlation with increases in its expression. Although *p21* is known to be regulated by epigenetic mechanisms (Bott *et al.*, 2005; Yoon *et al.*, 2012), including DNA methylation and histone modifications, almost all of these data have focused on epigenetic changes of *p21* in cancer cells (Bott *et al.*, 2005; Moreira *et al.*, 2009; Teramen *et al.*, 2011; Ying *et al.*, 2004). In contrast, a gap-in-knowledge exists with regard to the epigenetic regulation of *p21* by environmental oxidants like BrO_3^- or any other DBPs.

Furthermore, evidence supporting a role for epigenetics in the toxicity of BrO_3^- is the fact that both the histone deacetylase (HDAC) inhibitor trichostatin A (TSA) and the DNA methyltransferase (DNMT) inhibitor 5-aza-2′-deoxycytidine (5-Aza) increased BrO_3^--induced cytotoxicity when compared with BrO_3^- or TSA and 5-Aza alone (Scholpa *et al.*, 2014). The increase in toxicity correlated with decreased p21. Although changes in p21 expression correlated with changes in *p21* DNA methylation, the specific CpG sites altered were not identified. We addressed this limitation in this study using a modification of the bisulfite amplicon sequencing (BSAS) methylation analysis approach called targeted gene bisulfite sequencing (TGBS).

Next-generation sequencing methods are more frequently used to assess methylation of whole-genomes, reduced representation of genomes, and target capture of many loci. Although these methods create a significant amount of data they can be somewhat complex, expensive and are not yet as amicable to studies testing multiple exposure and doses of toxicants. Thus, simple, flexible, and low-cost methods are needed to leverage NGS for sequencing single-locus amplicons from large numbers of samples. We developed TGBS as a 2-stage PCR approach for rapid analysis of DNA methylation of targeted loci. TGBS differs from most of the current next-generation bisulfite sequencing approaches, including reduced representation bisulfite sequencing and BSAS, which typically perform whole-genome or target-gene fragmentation during library preparation (Kruger *et al.*, 2012; Masser *et al.*, 2013; Meissner *et al.*, 2005). These approaches have limitations in terms of inconsistent fragment lengths, complicated sequence mapping and methylation analysis. TGBS does not rely on fragmentation and because each amplicon is its own read, the library preparation and data analysis are comparatively simplified. We recently demonstrated the ability of TGBS to assess *p21* DNA methylation in renal cells in response to 5-Aza (Scholpa *et al.*, 2016).

In addition to DNA methylation, histone acetylation/deacetylation is also believed to play a key role in *p21* regulation in cancer cells (Shin *et al.*, 2000; Sowa *et al.*, 1997). For example, treatment of human colon cancer cells with HDAC inhibitors TSA or sodium butyrate increased the transcription of *p21* by inducing the acetylation of histones H4 and H3 (Fang *et al.*, 2004). We recently showed that TSA increases p21 protein expression in renal cells (Scholpa *et al.*, 2014) by increasing the acetylation of lysine 9 and 14 on histone H3 (H3K9/14 Ac) (Scholpa *et al.*, 2016). However, the effects of BrO_3^- on H3K9/14 Ac levels at the *p21* promoter region are not known. We also showed the DNMT inhibitor 5-Aza increased p21 expression in rat and human renal cells (Scholpa *et al.*, 2014), but similar to our studies with TSA, the exact site targeted by 5-Aza are not known. In this study, we address this gap-in-knowledge using TGBS and show that substantial differences exist in the basal methylation of the promoter regions of rat and human *p21*. We then determined the effect of BrO_3^- on this methylation. We also identified changes in H3K9/14 Ac levels after sub-chronic exposure of HEK293 and normal rat kidney (NRK) cells to low doses of BrO_3^- using chromatin immunoprecipitation (ChIP). Data derived from these studies are critical for understanding the role of epigenetics in the toxicity of BrO_3^- and in understanding the molecular mechanism by which nephrotoxicants and epigenetics regulate *p21*, a critical nephroprotective gene.

MATERIALS AND METHODS

Normal rat kidney cells, human embryonic kidney cells (HEK293), and penicillin and streptomycin were purchased from American Type Culture Collection (Manassas, Virginia). Human proximal tubule (hPT) cells were derived from whole, de-identified human kidneys that were obtained through the International Institute for the Advancement of Medicine (Edison, New Jersey). All tissue was scored by a pathologist as normal (ie, derived from noncancerous, nondiseased tissue). Potassium bromate ($KBrO_3$), 5-Aza, TSA, trypsin EDTA, glycine, and 37 wt.% formaldehyde were purchased from Sigma-Aldrich (St. Louis, Missouri), Dulbecco's modified Eagle medium (DMEM) was purchased from HyClone technologies (Logan, Utah), 5-Aza was dissolved in dimethyl sulfoxide (DMSO) from Fisher Scientific (Pittsburg, Pennsylvania). DNeasy blood and tissue extraction kit was purchased from Qiagen (Valencia, California). The EZ-DNA methylation lightning kit was purchased from Zymo research (Irvine, California). The nucleospin gel and PCR clean-up kit was purchased from Macherey-Nagel (Düren, Germany). The EpiQuik acetyl-histone H3 ChIP kit was purchased from Epigentek (Farmingdale, New York). The PCR master mix was purchased from Promega (Madison, Wisconsin) for ChIP-PCR. The MiSeq reagent v3 kit was purchased from Illumina, Inc. (San Diego, California), the Kapa HiFi PCR kit from Kapa Biosystems (Wilmington, Massachusetts), and the Maxima hot-start taq DNA polymerase for bisulfite-PCR and the Sera-Mag magnetic speedbeads were purchased from Thermo Scientific (Waltham, Massachusetts).

Cell Culture and Sub-chronic Treatment

5-Aza and TSA were used as positive controls. 5-Aza is a DNA methyltransferase inhibitor used in many studies for its demethylating properties (Bott *et al.*, 2005; Broday *et al.*, 1999; Christman, 2002; Shin *et al.*, 2000). TSA is a HDAC inhibitor and

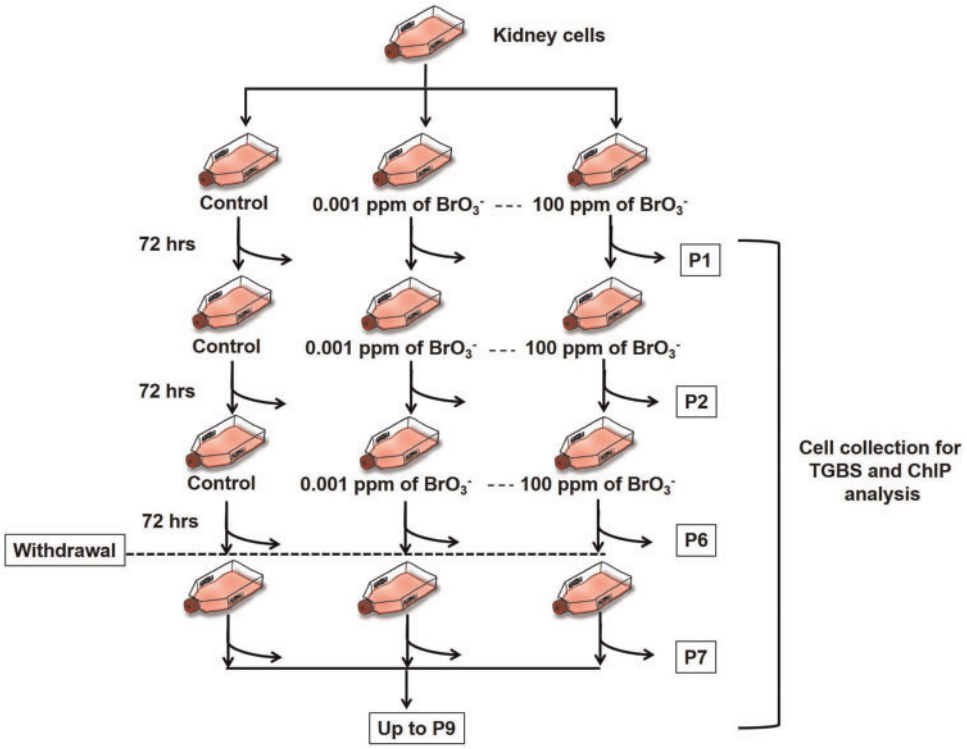

Figure 1. Sub-chronic dosing regimen for BrO_3^- and epigenetic inhibitors. Cells were exposed to various concentrations of BrO_3^- at log phase (after 24 h of seeding) for 72 h. A portion of the cells was used for reseeding and the rest for sample collection for targeted gene bisulfite sequencing and chromatin immunoprecipitation. This was called passage 1 (P1) and the regimen continued until 18 days (P6). Cells were allowed to recover by discontinuing the exposures for the next 3 passages (Days 21–27 or P7–P9) to obtain withdrawal samples.

used widely to study anticancer and anti-inflammatory mechanisms (Adcock, 2007; Drummond *et al.*, 2005; Vanhaecke *et al.*, 2004). HEK293 cells (3×10^6) were seeded in T-175 tissue culture flasks and NRK cells (1.5×10^6) were seeded in T-75 flasks and grown at 37°C in a 5% CO_2 incubator. Cells were treated with 0–100 ppm bromate (BrO_3^-), 40 μM 5-Aza, 100 nM TSA, or 0.05% DMSO (vehicle control for TSA and 5-Aza) for 72 h at log phase (after 24 h of seeding). A portion of the cells was used for reseeding and the rest for sample collected for TGBS or ChIP. The first set of samples was collected from passage 1 (P1) of the sub-chronic regimen, which was continued for 18 days (P6), ie, the cells were treated for 18 days and passaged every 3 days for sample collection. The rationale for this regimen is explained in our previous studies (Scholpa *et al.*, 2014, 2016; Zhang *et al.*, 2010, 2011). In short, we designed *a* sub-chronic *in vitro* regimen to obtain the environmentally relevant concentrations and exposures of bromate. Bromate in most drinking waters ranges from 0.001 to 0.1 ppm, which is the key range in our study with a continuous exposure of 18 days with a cell passage every 3 days. Unlike our previous studies, dosing in this study was followed by withdrawal studies where the exposure to BrO_3^- or the epigenetic inhibitors were discontinued for 9 days (P7–P9). This sub-chronic regimen is illustrated in Figure 1.

The procedure for isolation of hPT cells was based on that originally described by Todd *et al.* (1996), modified (Cummings and Lash, 2000; Cummings *et al.*, 2000) and reported in Huang *et al.* (2015). Briefly, sterile conditions (ie, all instruments and glassware were autoclaved, and all buffers were filtered through a 0.2 μm pore-size filter) were used. The renal cortex and outer stripe were cut into slices, washed with sterile PBS, minced, and the pieces were placed in a trypsinization flask filled with 300 ml of sterile, filtered Hanks' buffer, containing 25 mM $NaHCO_3$, 25 mM HEPES, pH 7.4, 0.5 mM EGTA, 0.2% (w/v) bovine serum albumin, 50 μg/ml gentamicin, 1.3 mg/ml collagenase, and 0.59 mg/ml $CaCl_2$, which was filtered prior to use. Whole kidneys were perfused with Wisconsin or similar type medium and kept on ice until they arrived at the laboratory, which was usually within 24 h of removal from the donor. All buffers were continuously bubbled with 95% O_2/5% CO_2 and were maintained at 37°C. Minced cortical pieces from whole kidneys were subjected to collagenase digestion for 60 min, after which the supernatant was filtered through a 70-μm mesh filter to remove tissue fragments, centrifuged at 150 × g for 7 min, and the pellet suspended in Dulbecco's Modified Eagle's Medium: Ham's F-12 (DMEM/F-12; 1:1). Approximately 5–7 $\times 10^6$ cells were obtained per 1 g of human kidney cortical tissue.

Targeted Gene Bisulfite Sequencing

The DNA methylation of *p21* promoter and coding regions in HEK293, NRK, and hPT cells was analyzed using TGBS, which is a modification of BSAS. Cells (5×10^6) were pelleted at 1000 rpm for 5 min and the supernatant was discarded. Genomic DNA was extracted using the Qiagen's DNeasy blood and tissue kit following the manufacturer's protocol. DNA was eluted in 2 successive steps to obtain a maximum yield, using 120 μl followed by 40 μl of elusion buffer. Following quantification using a Nanodrop spectrophotometer, 2 μg of the extracted DNA was bisulfite treated using the Zymo Research's EZ-DNA methylation lightning kit following the manufacturer's protocol, and requantified.

Bisulfite converted DNA (350 ng) was used to amplify different regions of the *p21* promoter. The locus-specific primers

Table 1. TruSeqHT Fusion Stubs and Locus-specific Primers for TGBS

Locus	Forward Primer (5′→3′)	Reverse Primer (5′→3′)	T_a[a] (°C)	Product Size (bp)
TruSeqHT fusion	iTru R1:ACACTCTTTCCCTACACGAC GCTCTTCCGATCT	iTru R2:GTGACTGGAGTTCAGACGTGT GCTCTTCCGATCT		
hp21-TSS[b]	ATAGTGTTGTGTTTTTTTGGAGAGTG	ACAACTACTCACACCTCAACTAAC	61.8	350
hp21-SIE1[c]	TTTTTTGAGTTTTAGTTTTTTTAGTAGTGT	AACCAAAATAATTTTTCAATCCC	61.8	335
rp21-coding[d]	TGTAATTAGTTATAGGTATTATGTTCGA	ACCCCTACAACAAAACCGAA	54.2	326
rp21-TSS[e]	TTTTTTATTTTTGGTTGTTTTTTTT	ACAAACAATTAACTCTCCTCAAATC	54.2	208

The iTru R1 or iTru5 fusion sequence was synthesized on the 5′ end of each of the 4 forward primers and the iTru R2 or iTru7 fusion sequence was synthesized on the 5′end of each of the 4 reverse primers.
[a]Annealing temperature.
[b]Human *p21* transcription start site.
[c]Human *p21* sis-inducible element-1.
[d]Rat *p21* coding region.
[e]Rat *p21* transcription start site.

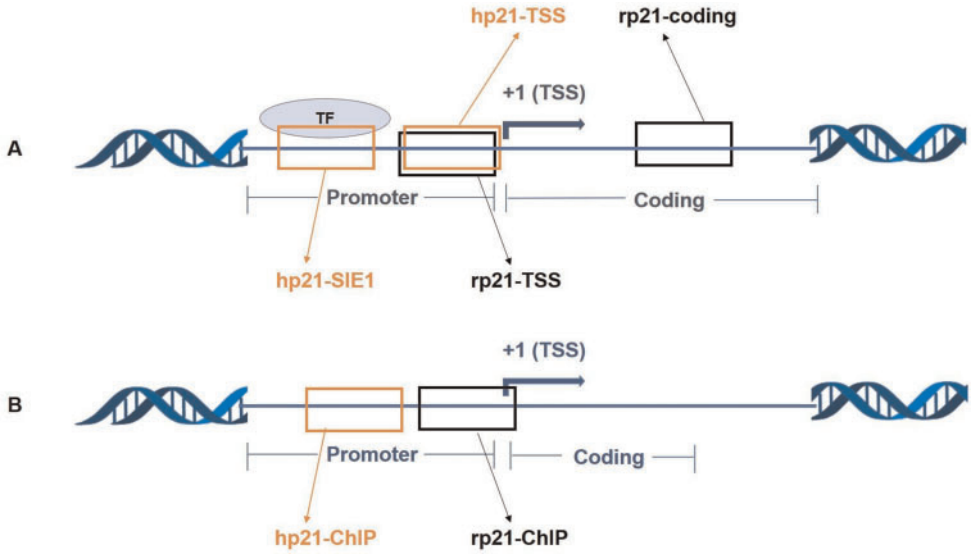

Figure 2. Schematic of *p21* gene organization highlighting the loci of interest for (A) DNA methylation analysis: the human *p21* promoter region adjacent to the transcription start site (hp21-TSS), the human transcription factor binding site called the sis-inducible element (hp21-SIE1), the rat *p21* promoter region starting near the start site (rp21-TSS), and the rat *p21* coding region (rp21-coding). (B) Histone acetylation analysis: the human *p21* promoter region (hp21-ChIP) about 1000 bp upstream of the transcription start site and rat *p21* promoter region (rp21-ChIP) at the TSS.

were designed using Methprimer (Li and Dahiya, 2002) and were synthesized by Integrated DNA Technologies, Inc (IDT, Coralville, Iowa). Partial TruSeqHT sequences corresponding to part of the Illumina Read1 (R1) and Illumina Read2 (R2) sequencing primer-binding sites (BadDNA, 2017; Faircloth and Glenn, 2012; Glenn *et al.*, 2016) were added 5′ to the locus-specific primers during primer synthesis. The locus-specific primers and the partial TruSeqHT sequences are listed in Table 1. Fusion primers were synthesized by IDT, where R1 was fused to forward primers and R2 was fused to reverse primers. For example, the primer pair for human *p21* TSS (hp21-TSS) was, forward: "iTru R1+hp21-TSS F" (ACACTCTTTCCCTACACGACGCTCTTCCGATCT ATAGTGTTGTGTTTTTTTTGGAGAGTG) and reverse: "iTru R2+hp21-TSS R"(GTGACTGGAGTTCAGACGTGTGCTCTTCCGAT CTACAACT ACTCACACCTCAACTAAC).

The first locus amplified was a 350 bp fragment of the human *p21* promoter region adjacent to the transcription start site (TSS) termed as hp21-TSS. The second locus was a 335 bp fragment including the transcription factor binding site approximately 700 bp upstream of the TSS called the sis-inducible element (SIE-1) and was termed hp21-SIE1. The third site was the 208 bp fragment of the rat *p21* promoter region near the TSS termed as rp21-TSS, and the 4th locus was the 326 bp rat *p21* coding region approximately 9 kb downstream of the TSS, termed rp21-coding. The schematic of these regions are shown in Figure 2A.

The 25 μl PCR amplification reaction mix contained 3 mM $MgCl_2$, 1X hot start buffer (Thermo Scientific), 0.2 mM of each deoxynucleoside 5′-triphosphate (dNTP), 0.4 μM each of the forward and reverse primers, 1.5 units HotStart Taq DNA polymerase (Thermo Scientific), and the 350 ng DNA template. PCR was performed under the following conditions: 95°C for 5 min, 40 cycles of 95°C for 30 s, 61.8°C (hp21-TSS or hp21-SIE1), or 54.2°C (rp21-TSS or rp21-coding) for 45 s followed by, 72°C for 45 s and a final 72°C for 10 min. The PCR products were then separated by electrophoresis on a 1% (w/v) agarose gel and visualized with ethidium bromide under a UV trans-illuminator and the amplicons corresponding to the loci were extracted from the gel using

Table 2. Primer Sequences for ChIP

Locus	Forward Primer (5′→3′)	Reverse Primer (5′→3′)	T_a[a] (°C)	Product Size (bp)	Reference
rp21-ChIP[b]	GTTCAGCCCTGGAACCGAAG	GTACCAAACACCCTTCACCTGGTAC	59	227	Yuan *et al.* (2013)
rGAPDH[c]	CACGGCAAGTTCAACGGCACAGTCA	GTGAAGACGCCAGTAGACTCCAGGAC	54.2	150	—
hp21-ChIP[d]	GGGGCTTTTCTGGAAATTGC	CTGGCAGGCAAGGATTTACC	54.2	116	Mitani *et al.* (2005)
hGAPDH[e]	AAGGTCGGAGTCAACGGAT	TGGAAGATGGTGATGGGATT	54.2	221	—

[a]Annealing temperature.
[b]Rat *p21* region analyzed using chromatin immunoprecipitation.
[c]Rat *GAPDH* = glyceraldehyde 3-phospate dehydrogenase, analyzed using chromatin immunoprecipitation.
[d]Human *p21* region analyzed using chromatin immunoprecipitation.
[e]Human *GAPDH* region analyzed using chromatin immunoprecipitation.

the Nucleospin gel and PCR clean-up kit (Macherey-Nagel) following the manufacturer's instructions. The sequences of the purified PCR products were confirmed using Sanger sequencing at the Georgia Genomics and Bioinformatics Core at the University of Georgia. All sequences obtained were verified for locus-specificity using the Basic Local Alignment Search Tool (Altschul *et al.*, 1990).

Purified PCR amplicons from agarose gel extraction were normalized to 5 ng/μl. A limited cycle PCR was performed to attach the iTru5 and iTru7 primers with 8 nucleotide indexes, as represented in Supplementary Figure 1. The 15 μl limited cycle reaction contained 1X Kapa buffer, 0.3 mM of each dNTP, 0.3 μM of each primer, 15 ng template DNA, and 0.3 U of HiFi HotStart DNA polymerase (Kapa Biosciences). The reaction conditions were: 98°C for 5 min, 11 cycles of 98°C for 15 s, 60°C for 30 s, and 72°C for 30 s and a final 72°C for 1 min. Aliquots (10 μl) from each reaction were pooled together and cleaned up using Thermo Scientific's Sera-Mag magnetic speedbeads. The pooling, cleaning, and processing of the sample for sequencing on an Illumina MiSeq platform using MiSeq 600 cycle v3 kit are as described by Glenn *et al.* (2016).

Sequence Analysis

Read quality and trimming. The paired end 250–350 bp reads obtained from Illumina MiSeq were demultiplexed using Illumina software bcl2fastq (Bcl2fastq2, 2013). The sequence reads in fastq format were trimmed for better alignment using Babraham Bioinformatics' free software Trim Galore (Trim Galore, 2012) or Geneious (Geneious, 2017; Kearse *et al.*, 2012). However, because the sequencing templates included mostly the uniformly sized gel extracted PCR products, trimming did not affect read alignment (data not shown).

DNA methylation analysis using bismark. Bismark bisulfite mapper is a Linux based free software from Babraham Bioinformatics Institute (Krueger and Andrews, 2011). Methylation analysis using Bismark was carried out in 3 steps:

- *Genome preparation*: A reference genome was prepared where a genome sequence from the National Center for Biotechnology Information (NCBI) for the target locus (*p21* promoter or coding region) was downloaded as a fasta file. The reference genome was prepared using the following command: "bismark_genome _preparation –/home/user/DNA/bowtie2-2.3.0/–verbose/home/user/DNA/bowtie2-2.3.0/bismark_v0.17.0/REF/," where the reference fasta file was saved in a directory or folder REF in the home folder of the user within the bismark folder. This created 2 folders within the genome folder REF, 1 with C ->T genome index and another with G ->A for the reverse reads.
- *Read alignment*: The second step was running bowtie2 within Bismark using the command: "bismark –bowtie2/home/user/DNA/bowtie2-2.3.0/bismark_v0.17.0/REF/SampleSeq_R1.fastq.gz," where read alignment for sequences in the folder named SampleSeq_R1 with a single-end approach was performed. This aligned the sequence reads to the reference genome and created a combined alignment or methylation call output in a binary representation of sequence alignment map called BAM and yielded a run statistics report. Output files included a bam file and report.txt file (Supplementary Datafile 1). The BAM file can only be opened in Bismark.
- *Methylation extraction*: The third and final step was methylation extraction of the bam file generated in the second step. The command used was "bismark_methylation_extractor -s –comprehensive SampleSeq_R1.fastq_bismark_bt2.bam." This generated output files that included M-bias.txt file, M-bias_R1.png file, CpG (Supplementary Datafiles 2–4), CHH and CHG context bt2.txt files, which contain information on strand-specific methylation. The key information on CpG site-specific percent methylation was obtained from the M-bias.txt file (Supplementary Datafile 2). The targeted bisulfite sequencing with short products allowed for manual extraction of methylation values for comparison across samples. A processing report was generated using the command "bismark2report" that summarized the process with a read alignment chart, methylation extraction report, and an M-bias plot.

VirtualBox With Ready-to-run Bismark Package

VirtualBox is an open source software that runs on various operating systems and supports various guest operating systems (VirtualBox, 2017). The path to download a ready-to-run VirtualBox package containing all the tools and installations required for DNA methylation analysis of a given fastq sequence file is indicated below. The package includes a working Bismark, which is a Linux software, in a VirtualBox on Windows host system. This can be found at "http://toxicology.uga.edu/resources/dna_methylation_analysis/" for the VirtualMachine named "TGBS" that can be accessed with the username "user" and password "TGBSKolli." The instructions are detailed in the Supplementary File.

Chromatin Immunoprecipitation

The effect of BrO_3^- on *p21* histone acetylation was investigated using Epigentek's EpiQuik acetyl-histone H3 ChIP kit based on the manufacturer's protocol with conditions optimized for HEK293 and NRK cells (Supplementary File). The primer sequences for ChIP-PCR are described in Table 2 and schematically represented in Figure 2B. The *p21* promoter regions selected previously showed TSA-induced hyperacetylation of lysine 9 and 14 on histone H3 (H3K9/14 Ac) in human gastric carcinoma

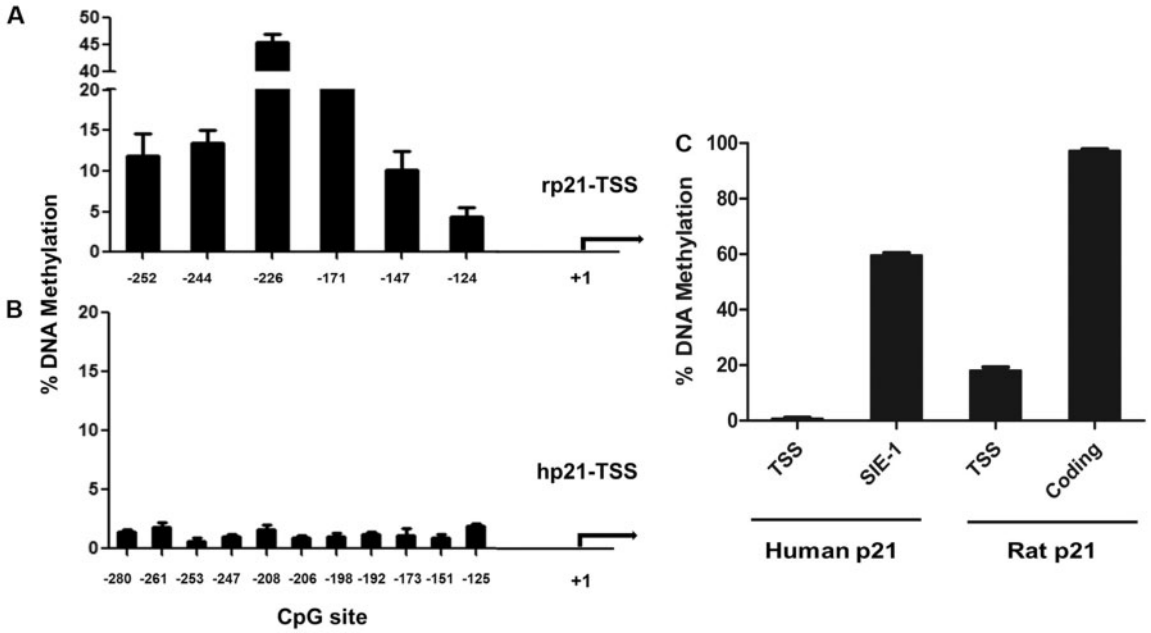

Figure 3. Differential methylation analysis. Comparison of methylation between rat (A) and human (B) *p21* transcription start sites. DNA methylation data are represented as the percent methylation of each CpG site in the analyzed fragments of the human and rat *p21* promoter regions near the respective transcription start sites (rp21-TSS and hp21-TSS). C, Comparison of methylation in different regions of the rat and human *p21* gene. Differential methylation data are represented as the percent DNA methylation of the transcription start site, sis-inducible element (SIE-1), and gene coding regions of human and rat *p21*. Next-generation sequencing data was analyzed using Bismark bisulfite mapper. Data are represented as the mean ± SEM of 3-independent experiments ($n = 3$).

cell lines (Mitani *et al.*, 2005) and rat mesangial cells (Yuan *et al.*, 2013). The human *p21* promoter analyzed was approximately 1000 bp upstream of the TSS (hp21-ChIP) and the rat *p21* promoter region at the TSS (rp21-ChIP).

Statistics

Samples isolated from a distinct cell passage represented 1 experiment ($n = 1$). Data are represented as mean ± SEM (standard error of the mean) from at least 3 separate experiments ($n = 3$). For cell number and histone acetylation data, an unpaired Student's *t* test was used to compare individual dose to the controls (each dose to the control). For the methylation data containing multiple exposures and multiple CpG sites, 2-way analysis of variance was used followed by Bonferroni post hoc test. Statistical analysis was performed using Graphpad PRISM considering $p < .05$ indicative of a statistically significant difference between the mean values.

RESULTS

Differences in Basal DNA Methylation of the p21 Promoter Region Between Human and Rat Kidney Cells

Prior to determining the effect of BrO_3^- on the methylation of *p21* we determined differences in basal DNA methylation between human and rat *p21* promoters isolated from HEK293 and NRK cells. The sites analyzed included a 350 bp upstream fragment of the human *p21* promoter adjacent to the TSS (hp21-TSS) and a 250 bp upstream fragment of the rat *p21* promoter near the TSS (rp21-TSS). The basal methylation of promoter CpG sites in the rat *p21* TSS was substantially higher than that measured in the human *p21* TSS (Figs. 3A and 3B). The average total DNA methylation at CpG sites in the rat p21 TSS was 16.4%, as compared with 0.8% in the human *p21* TSS (Figure 3C). In contrast, the average methylation of CpG site in the SIE-1 promoter site in human *p21* was almost 60%. The methylation of CpG sites in the rat *p21* coding region (rp21-coding) was also assessed as a control (Figure 3C). We have previously used methylation-specific PCR to show that this site was highly methylated (Scholpa *et al.*, 2014). As expected, the average methylation at this site was almost 100%.

Regional Differences in Basal DNA Methylation of p21 Between HEK293 Cells and Freshly Isolated Human Proximal Tubule Cells

Having established differences in the basal methylation between the rat and human *p21* promoter regions we expanded our analysis to differences in CpG methylation between renal cells from the same species. The regions analyzed were the human *p21* TSS and the SIE-1 site of human *p21* promoter (hp21-SIE1) as shown in Figure 2A. We investigated the differences in basal level methylation of these regions between HEK293 cells and freshly isolated hPT. The average methylation of human *p21* TSS in hPT cells was 1.4% and was not significantly different from that in HEK293 cells (Figure 4A). In contrast, the average methylation of all 3 CpG sites of the human *p21* SIE1 site at 691 and 855 bp upstream of the human *p21* TSS in hPT cells were significantly lower than that measured in HEK293 cells (Figure 4B).

Effect of BrO_3^- on Cell Number and Morphology

Having established the differences in methylation between rat and human *p21*, we next investigated the effects of sub-chronic exposure of renal cells to environmentally relevant concentrations of BrO_3^- on *p21* DNA methylation and histone acetylation. Our previous study (Scholpa *et al.*, 2014) demonstrated concentrations of BrO_3^--induced p21 expression as early as 3 days of exposure at all doses tested including 0.01 ppm. In this subchronic study, we hypothesized that these changes in p21 expression are a result of epigenetic mechanisms. To test the general premise of stability of these epigenetic changes, we

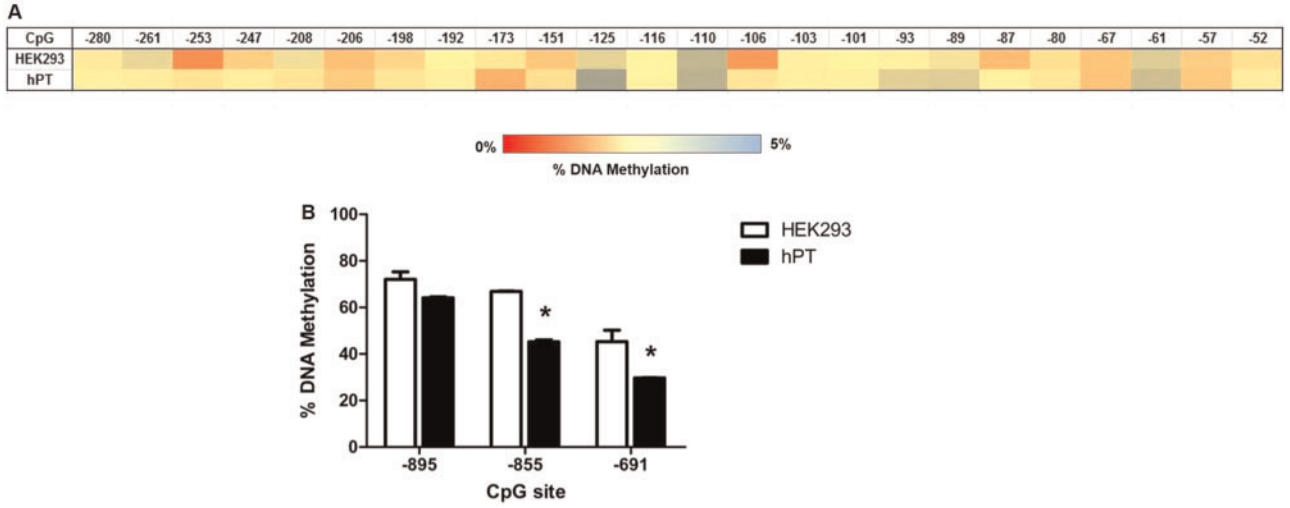

Figure 4. Comparison of basal DNA methylation of the *p21* promoter region between HEK293 cells and freshly isolated human proximal tubule (hPT) cells. (A) Heat map of the site-specific percent DNA methylation changes as determined by targeted gene bisulfite sequencing in the human *p21* promoter region at the transcription start site (hp21-TSS). (B) Comparison of methylation of human *p21* promoter at the transcription factor binding site SIE-1 between HEK293 and hPT cells. Data are represented as the mean ± SEM of 3 different passages of HEK293 cells and 3 different pools of freshly isolated hPT cells ($n = 3$). *$p < .05$ compared with HEK293.

introduced an extra 9 days of withdrawal studies where the cells did not receive doses of BrO_3^- or epigenetic inhibitors.

In agreement with our previous study (Scholpa *et al.*, 2014), treatment of HEK293 cells with doses of BrO_3^- below 100 ppm did not significantly alter cell morphology or number after 18 days of treatment (Figs. 5A–F and 5J). We also did not observe significant alterations in cell number or morphology of the cells after 9 days of withdrawal (Figs. 6A–F and 6J). Similar results were seen with NRK cells (Supplementary Figs. 2 and 3). In our acute study, cells treated with 100 ppm BrO_3^- showed initial signs of cell rounding, detachment and small decreases in cell number compared with the control cells after 3 days (data not shown). We could not study the sub-chronic effect of 100 ppm BrO_3^- past 6 days (P2) in HEK293 cells and past 9 days (P3) in NRK cells due to further toxicity that correlated with an immense decrease in cell number. These data agree with our previous studies that the lower doses of BrO_3^- used in this study do not induce detectable levels of cell death (Scholpa *et al.*, 2014).

Exposure of HEK293 cells to 40 μM 5-Aza altered cell morphology and cell number after 3 days, a trend that continued through the 18 days of exposure (Figs. 5I and 5J). This morphology and number recovered after 9 days of withdrawal but were still significantly different from the DMSO withdrawal cells (Figs. 6I and 6J). Exposure of cells to 100 nM TSA did not alter cell morphology or number after 18 days of sub-chronic treatment. Similar results were observed in NRK cells with BrO_3^- and the epigenetic inhibitors (Supplementary Figure 2).

Effect of BrO_3^- on p21 Promoter Methylation

Our previous studies (Scholpa *et al.*, 2014) demonstrated changes in *p21* methylation in the coding regions that correlated with sub-chronic exposure to environmentally relevant concentrations of BrO_3^-. Despite these data, the changes in methylation in the promoter region of *p21* were not assessed nor were differences between rat and human *p21*. Furthermore, the exact CpG sites targeted were not identified. We addressed this gap-in-knowledge by analyzing DNA methylation of *p21* in both rat and human renal cells exposed to BrO_3^- at concentrations that did not induce detectable cell death. The regions analyzed were the same 350 bp fragment of the human *p21* TSS comprising 24 CpG sites, a 335 bp fragment including the human *p21* SIE1 consisting 3 CpG sites at 691, 855, and 895 bp upstream of the TSS, a 250 bp fragment of the rat *p21* TSS comprising 6 CpG sites and the rat *p21* coding region approximately 9 kb downstream of the TSS with 21 CpG sites. We also assessed the effect of 5-Aza as a positive control.

Neither 5-Aza nor BrO_3^- (0.001–10 ppm) altered DNA methylation after acute (Supplementary Figure 4) and sub-chronic exposure (Supplementary Figure 5) at the human *p21* TSS in HEK293 cells and at rat *p21* coding region in NRK cells (Supplementary Figure 6). These concentrations and exposure times had been shown to induce p21 protein expression in these cells (Scholpa *et al.*, 2014). However, 5-Aza decreased DNA methylation at 2 CpG sites in the human *p21* SIE1 site after 3 and 9 days of exposure (Figs. 7A–D). In contrast, BrO_3^- had no effect on the methylation of the CpG sites at any concentration or exposure. The decrease in DNA methylation induced by 5-Aza was greater after 18 days of exposure at all 3 CpG sites, as compared with 9 days (Figs. 7E and 7F). Similar decrease was observed in NRK cells. 5-Aza decreased DNA methylation at the rat *p21* TSS after 9 days of exposure and BrO_3^- again did not alter methylation at these same sites in rat *p21* (Supplementary Figs. 7A and 7B). Withdrawal of 5-Aza for 9 days did not result in a return of DNA methylation to control levels at CpG site −895 and −855 in the human *p21* SIE1 site (Figs. 7G and 7H). Decreased methylation induced by 5-Aza was also observed at the CpG sites −226 and −171 in the rat *p21* TSS in NRK cells after withdrawal (Supplementary Figs. 7C and 7D). These data suggest that the effect of 5-Aza on DNA methylation at these sites had some permanence.

Effect of BrO_3^- on p21 Promoter Histone Acetylation

In the absence of changes in DNA methylation we investigated the hypothesis that changes in p21 expression induced by BrO_3^- were mediated by histone acetylation. This hypothesis is supported by our previous studies showing that treatment of HEK293 and NRK cells with the HDAC inhibitor TSA upregulated p21 protein expression (Scholpa *et al.*, 2014). We also

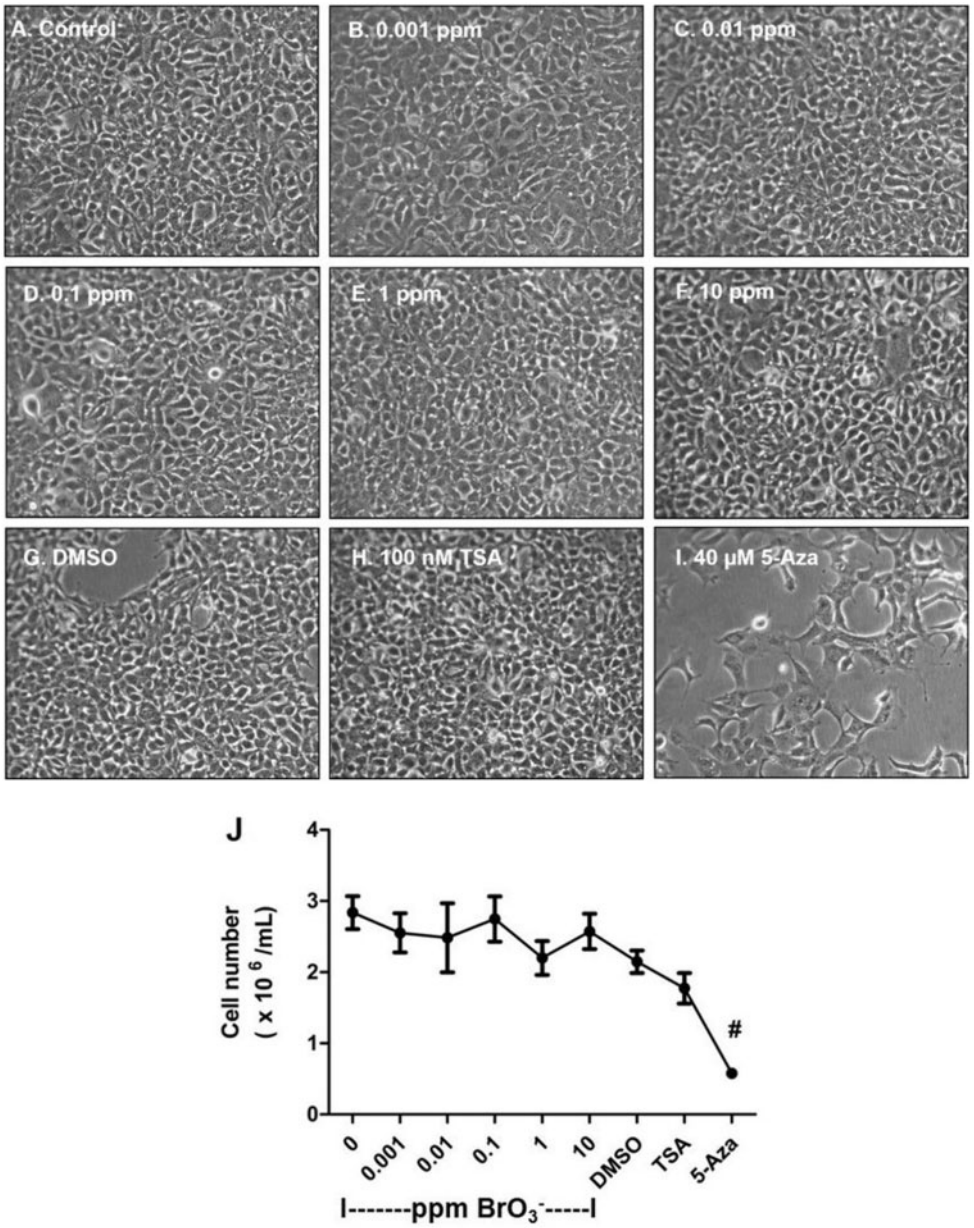

Figure 5. Sub-chronic effect of BrO_3^- and epigenetic inhibitors on HEK293 cell morphology and number. HEK293 cells were sub-chronically exposed to 0–10 ppm BrO_3^- (A–F), vehicle control dimethyl sulfoxide (DMSO) (G), 100 nM TSA (H), or 40 μM 5-Aza (I) for 18 days (P6). The cell number data in (J) are represented as mean ± SEM of 3 separate passages ($n = 3$). $^{\#}p < .05$ compared with DMSO.

demonstrated that TSA-induced p21 expression correlated with the increased acetylation of lysine 9 and 14 on histone H3 (H3K9/14 Ac) in the *p21* promoter region (Scholpa *et al.*, 2016). However, we do not know the effect of short- and long-term exposure of BrO_3^- on these cells, nor do we know the persistence of these changes.

Acute exposure (3 days or P1) of renal cells to 0.001–100 ppm BrO_3^- and 100 nM TSA did not affect the H3K9/14 Ac levels of the human *p21* promoter approximately 1000 bp upstream of the TSS (hp21-ChIP) but did alter acetylation in the rat *p21* promoter at the TSS (rp21-ChIP) at concentrations of 0.001 and 1 ppm BrO_3^- in a concentration-independent manner (Figure 8A). The sub-chronic effects of BrO_3^- and the positive control TSA were assessed at 9 days (P3), 18 days (P6), and 27 days (P9). Treatment of NRK cells with 0.001–10 ppm BrO_3^- or 100 nM TSA significantly increased H3K9/14 Ac levels of rat *p21* promoter after 9 days (P3) (Figure 8B). Similar increases were observed after 18 days (P6) of treatment with 0.01–10 ppm BrO_3^- (Figure 8C). Withdrawal of BrO_3^- for 9 (P9) days resulted in a return of H3K9/14 acetylation to control levels (Figure 8D). This same reversion was seen in cells exposed to TSA. To understand the time-dependence on this reversion, we assessed the recovery of the acetylation mark after 3 days of withdrawal (P7), which was long enough to result in a decrease in acetylation comparable with controls (Supplementary Figure 8). In contrast to NRK cells, H3K9/14 acetylation in HEK293 cells at the promoter site was not altered by BrO_3^- or TSA at any concentration and time point measured (Supplementary Figure 9).

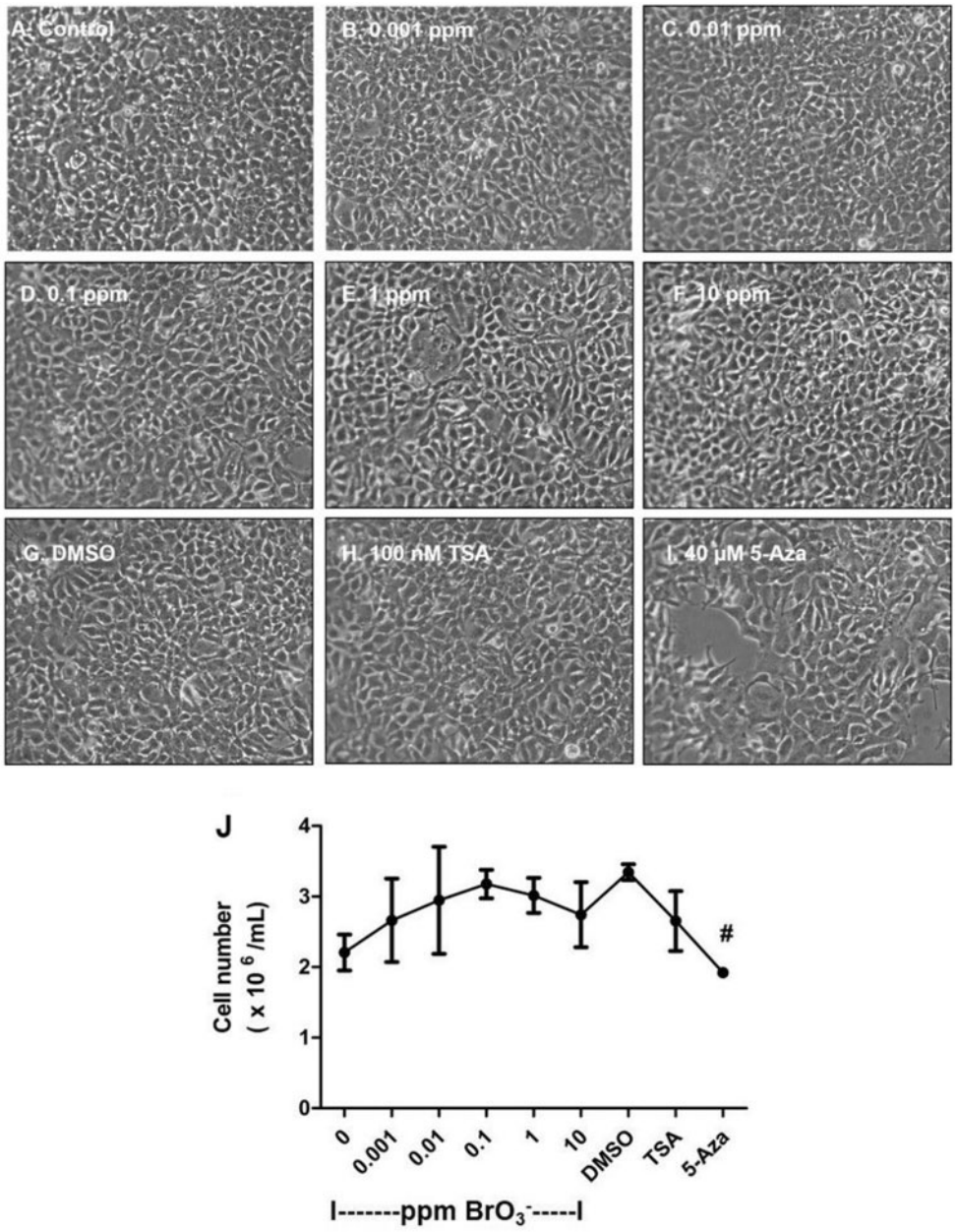

Figure 6. Effect of BrO_3^- and epigenetic inhibitors on HEK293 cell morphology and number after withdrawal. HEK293 cells were sub-chronically exposed to BrO_3^- for 18 days and then allowed to recover (A–F), vehicle control dimethyl sulfoxide (DMSO) (G), 100 nM TSA (H), or 40 μM 5-Aza (I) for 9 days (P9). The cell number data in (J) are represented as mean ± SEM of 3 separate passages ($n = 3$). $^{\#}p < .05$ compared with DMSO.

DISCUSSION

One of the primary goals of this study was to determine the ability of the DBP BrO_3^- to induce epigenetic changes in the nephroprotective gene *p21*. Understanding the molecular effect of BrO_3^-, especially at the epigenetic level, in renal cells is important as this chemical is a probable human carcinogen (IARC, 1999), and is reported to induce renal cancer in both rats and mice (Kurokawa *et al.*, 1990; Wolf *et al.*, 1998). Although the ability of DBPs, including BrO_3^-, to induce epigenetic changes has been studied previously, such studies use high non-environmentally relevant doses as well as acute exposure protocols. Data in this study demonstrate that BrO_3^- can induce changes in histone acetylation at doses as low as the MCL. These data also suggest that changes in p21 expression in both rat and human cells are not mediated by changes in methylation at the CpG sites in the promoter region of *p21*. It is possible that changes in DNA methylation may be occurring at sites distal to the TSS.

Data from these studies also identify 3 hitherto unidentified CpG sites in human *p21* promoter that are targeted by DNA methyltransferase. As previously reported, 5-Aza, an inhibitor of DNA methyltransferases, induced p21 expression in human renal cells but the exact CpG sites involved were not identified (Scholpa *et al.*, 2014). This study showed that 5-Aza significantly decreased percent methylation at the human *p21* SIE1 site in HEK293 cells, and that this decrease was enhanced after 18 days of sub-chronic exposure. Furthermore, and more importantly, decreased methylation persisted for 9 days after the withdrawal

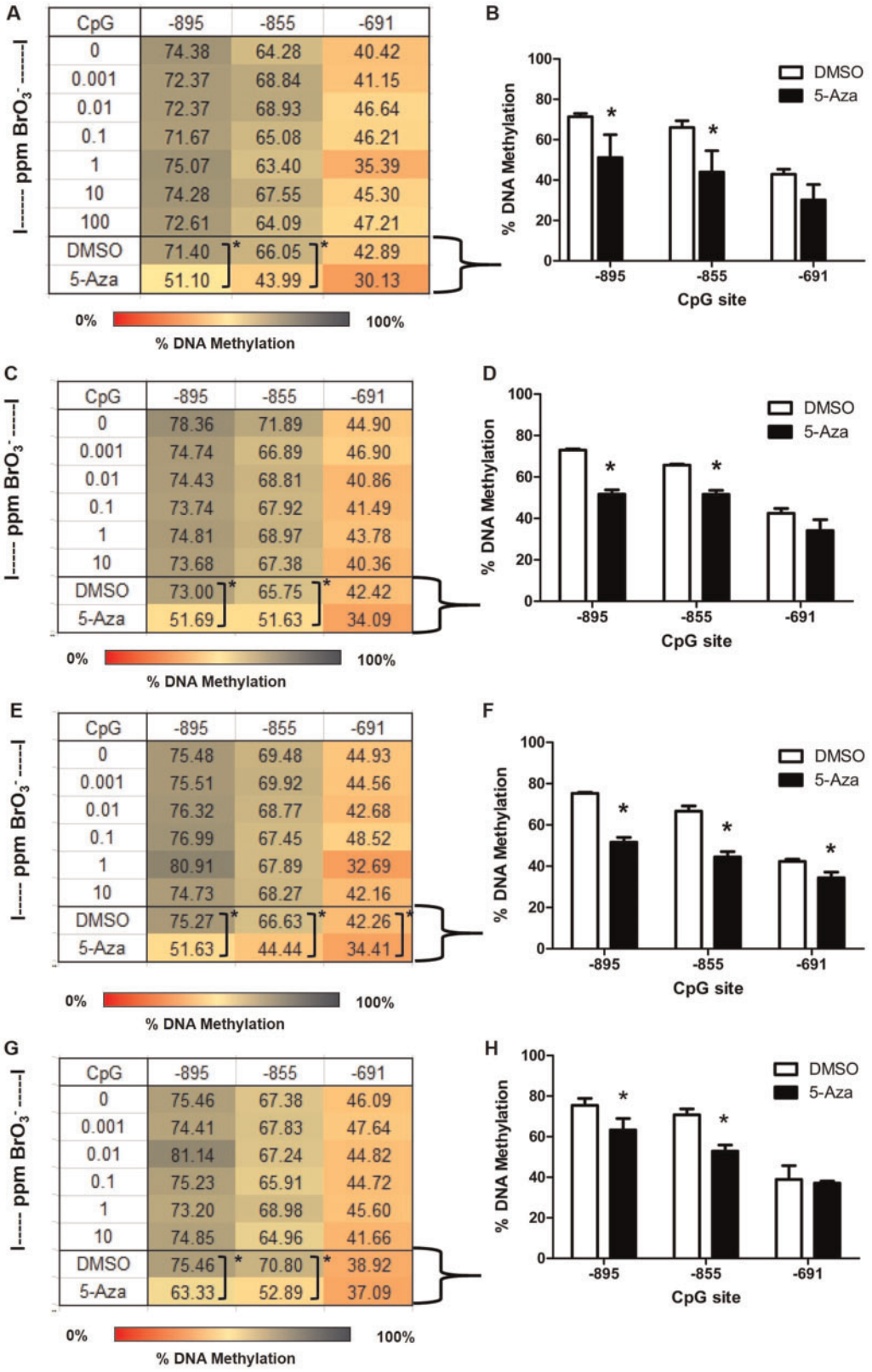

Figure 7. Acute and sub-chronic effects of BrO_3^- on the percent DNA methylation of CpGs in the SIE-1 site of the human *p21* promoter. HEK293 cells were treated with water (vehicle control for BrO_3^-), 0.001–100 ppm BrO_3^-, dimethyl sulfoxide (DMSO) (vehicle control for 5-Aza) or 40 μM 5-Aza (positive control) for 3 days or P1 (A and B), 9 days or P3 (C and D), 18 days or P6 (E and F). The cells were allowed to recover by discontinuing the exposures for 9 days or P9 (G and H). The first row in the heat map represents the position of the cytosine in the CpG dinucleotide context relative to the transcription start site. Data are represented as the average percent DNA methylation of 3 separate passages ($n = 3$) as determined by targeted gene bisulfite sequencing analysis. The effects of 5-Aza are emphasized in the bar graphs for the respective exposure times. Data are represented as the mean ± SEM of 3 different passages ($n = 3$). *$p < .05$ compared with DMSO.

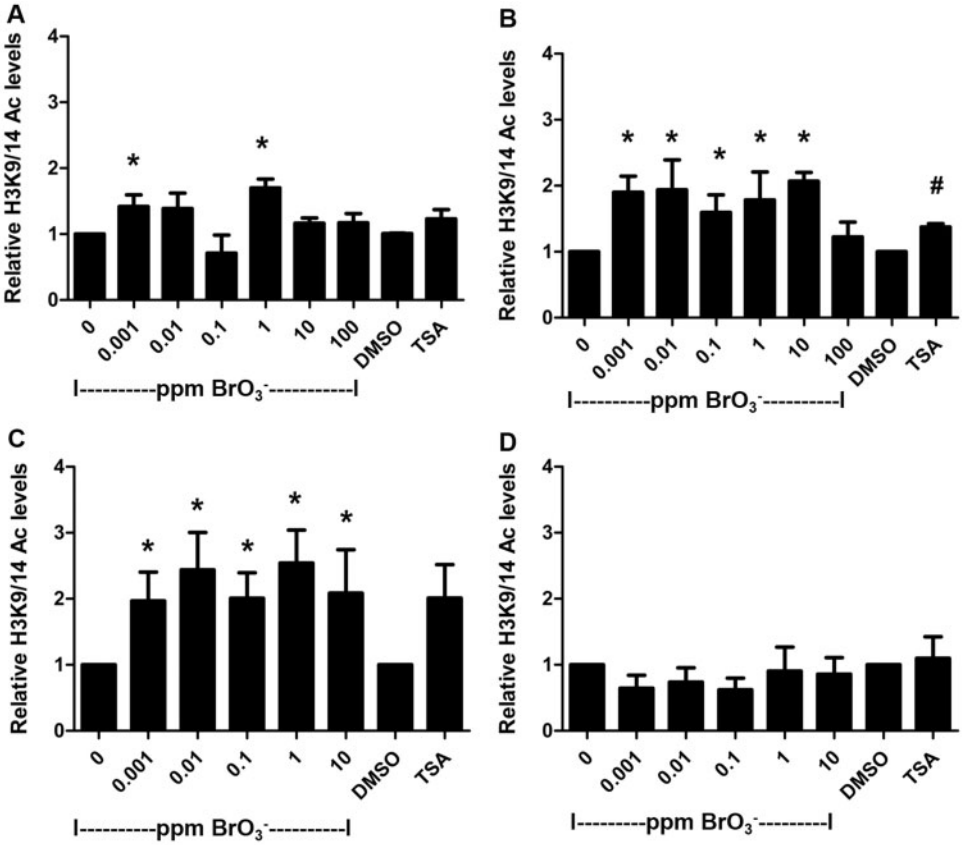

Figure 8. Sub-chronic effects of BrO_3^- on acetylation of lysine 9 and 14 on histone H3 (H3K9/14 Ac) of the rat *p21* promoter region. Normal rat kidney cells to were exposed to 0.001–100 ppm BrO_3^- for 3 days or P1 (A), 9 days or P3 (B), and 18 days or P6 (C). The cells were allowed to recover by discontinuing exposures for 9 days or P9 (D). Data are represented as the relative fold increase in H3K9/14 Ac levels as normalized to *GAPDH* as determined using the chromatin immunoprecipitation assay. Data are represented as the mean ± SEM of 3 different passages ($n = 3$). $^*p < .05$ compared with 0 ppm BrO_3^- and $^\#p < .05$ compared with DMSO.

of 5-Aza, which involved 3 passages of the cells. This supports the conclusion that changes in methylation at the CpG sites identified are true epigenetic changes. These CpG sites encompass an SIE-1 site. This site is recognized by members of the signal transducer and activator of transcription family. The binding of STAT1 protein to SIE-1 has also been shown to upregulate *p21* expression (Chin *et al.*, 1996). Our data suggest that the SIE-1 is an important region for epigenetic regulation of p21 expression. However, our data also suggest that BrO_3^- itself does not target this region.

It is important to point out that even though BrO_3^- failed to alter DNA methylation within the promoter region of either HEK293 or NRK *p21* does not suggest that DNA methylation is not involved in the regulation of p21 by BrO_3^-. Rather, it suggests that changes in DNA methylation at these specific sites are not involved. It is quite possible that changes in methylation at sites distant from the promoter region mediate p21 expression. Our choice for the sites analyzed with TGBS is obvious as these sites are within the promoter region. Future studies are needed to address the above hypothesis.

In contrast to methylation, BrO_3^- clearly altered histone acetylation. These data agree with that from Fang *et al.* (2004) who previously reported that histone acetylation regulates *p21* expression in many cancer cell lines. Shin *et al* (2000) also showed that *p21* promoter region was not methylated in gastric cancer cells but was regulated by histone deacetylase 1 (Shin *et al.*, 2000). Various studies, including ours (Scholpa *et al.*, 2014), reported that inhibition of HDAC increases p21 expression, including that induced by azelaic bishydroxamic acid (Burgess *et al.*, 2001), *n*-butyrate (Dagtas *et al.*, 2009), suberoylanilide hydroxamic acid (Gui *et al.*, 2004; Richon *et al.*, 2000), and statins (Lin *et al.*, 2008). The novelty in this study is that this is one of the first report to demonstrate that BrO_3^- exposure increases H3K9/14 acetylation. Furthermore, this study is the first to identify the location of this acetylation. Of further interest is that changes in acetylation occurred at doses as low as the EPA limit (0.01 ppm). The fact that changes in acetylation occurred in the absence of cell death, and that these changes were not persistent supports the hypothesis that induction of p21 after exposure to BrO_3^- is a protective rather than a toxic response. Further strengthening our previous observation that the role of p53 is key to the difference in the protective effect and the toxic effect of p21. At environmentally relevant doses p21 is activated independently of p53, at higher acutely toxic doses p53 is activated (Scholpa *et al.*, 2014). Another interesting finding from these studies is that BrO_3^- did not alter H3K9/14 acetylation in HEK293 cells. Data on the effect of both TSA and BrO_3^- on acetylation of H3K9/14 further support the hypothesis that epigenetic regulation of *p21* is species-dependent.

It should be noted that histones are modified by marks like lysine methylation, arginine methylation and citrullination, serine, tyrosine or threonine phosphorylation, and that we have only assessed lysine acetylation on histone H3. It is possible

that the lack of histone acetylation in human *p21* in response to BrO_3^- may be a result of acetylation at different histones within the promoter region, or a different modification at a different location in the noncoding region. Nevertheless, such data would still support the premise that epigenetic regulation of *p21* is species-dependent.

A major finding from these studies is that the basal DNA methylation of the promoter region of rat and human *p21* are substantially different. This can be highlighted by the fact that the overall methylation of CpG sites in human *p21* was about 10-fold lower than that measured in the similar region in rat *p21*. Furthermore, the promoter region of human *p21* also contains a SIE-1 site not present in rat. These data demonstrate that the epigenetic landscape of the promoter region of rat and human *p21* are not the same. The implication for this finding is that studies assessing the ability of nephrotoxicants to regulate p21 in rodent renal cells may not be comparable with human renal cells. As such, care should be taken in extrapolating epigenetic data, at least for BrO_3^- and *p21*, between species. Furthermore, this suggests that studies in human cells may be more relevant for such extrapolation and that changes in rat epigenetics in *p21* may not be as relevant. It's possible that epigenetic changes in other rat genes may mirror that of humans. Thus, we are unable to speculate globally if epigenetic effects should be studied for bromate.

Another interesting finding from these data is that the degree of basal DNA methylation of the promoter region of human *p21* varied between cell types. This is demonstrated by the fact that the level of DNA methylation at the CpG sites −855 and −691 were significantly lower in hPT cells compared with HEK293 cells. These data suggest that basal DNA methylation may not only differ between species, but also different between similar cell types from the same species. Further studies are needed to confirm this hypothesis. It should be noted that hPT cells used in this study were freshly isolated from whole tissue. That is not the case for HEK293 cells, which are immortalized and grown in media and are embryonic in origin. Thus, it is possible that the culture conditions may mediate changes in basal DNA methylation in the *p21* promoter region. It is reasonable to expect differences in basal DNA methylation between cell lines and freshly isolated cells. At the same time, it is known that the methylome of embryonic and adult cells are different irrespective of tissue type (Varley *et al.*, 2013). The toxicological manifestation of these differences is yet to be investigated. However, a limitation of this study is that epigenetic comparisons were made between human embryonic cell line and rat adult cell line. Future studies are needed to address this gap in knowledge. Regardless, these data suggest that epigenetic studies on the same gene may not translate from cell line to cell line, even within the same species.

In conclusion, our data demonstrate that the expression of rat p21 is regulated by histone acetylation and not DNA methylation in the regions analyzed, after sub-chronic exposure of rat renal cells to BrO_3^-. In contrast, it appears that while sites for epigenetic regulation do exist within the promoter regions of human and rat *p21*, these sites exist at different regions of the respective promoters. These data also demonstrate that DNA methylation within the promoter sites does not appear to mediate changes in expression of either rat or human p21 in response to BrO_3^-. Finally, these data demonstrate the species-specific differences in the epigenetic regulation of p21 and suggest an uncertainty in extrapolating rat epigenetic data for assessing the risk of toxicants in humans.

DECLARATION OF CONFLICTING INTERESTS

The author(s) declared no potential conflicts of interest with respect to the research, authorship, and/or publication of this article.

SUPPLEMENTARY DATA

Supplementary data are available at *Toxicological Sciences* online.

ACKNOWLEDGMENTS

We thank everyone involved in the generation of data. We thank Troy J. Kieran and Patrick R. Watson (T.C.G. laboratory) for their help in sample pooling and MiSeq runs.

FUNDING

This project was supported in part with funds from the National Institutes of Health (NIH); National Institute of Biomedical Imaging and Bioengineering (NIBIB) (EB0160100 to B.S.C.), as well as Interdisciplinary Toxicology Program Stipend Support and US-EPA's Student Services Authority Support to R.T.K.

REFERENCES

Adcock, I. M. (2007). HDAC inhibitors as anti-inflammatory agents. *Br. J. Pharmacol.* **150**, 829–831.

Altschul, S. F., Gish, W., Miller, W., Myers, E. W., and Lipman, D. J. (1990). Basic local alignment search tool. *J. Mol. Biol.* **215**, 403–410.

Bott, S. R., Arya, M., Kirby, R. S., and Williamson, M. (2005). P21WAF1/Cip1 gene is inactivated in metastatic prostatic cancer cell lines by promoter methylation. *Prostate Cancer Prostatic Dis.* **8**, 321–326.

Broday, L., Lee, Y. W., and Costa, M. (1999). 5-Azacytidine induces transgene silencing by DNA methylation in Chinese hamster cells. *Mol. Cell. Biol.* **19**, 3198–3204.

Burgess, A. J., Pavey, S., Warrener, R., Hunter, L. J., Piva, T. J., Musgrove, E. A., Saunders, N., Parsons, P. G., and Gabrielli, B. G. (2001). Up-regulation of p21(WAF1/Cip1) by histone deacetylase inhibitors reduces their cytotoxicity. *Mol. Pharmacol.* **60**, 828–837.

Chin, Y. E., Kitagawa, M., Su, W. C., You, Z. H., Iwamoto, Y., and Fu, X. Y. (1996). Cell growth arrest and induction of cyclin-dependent kinase inhibitor p21 WAF1/Cip1 mediated by stat1. *Science* **272**, 719–722.

Christman, J. K. (2002). 5-Azacytidine and 5-aza-2′-deoxycytidine as inhibitors of DNA methylation: Mechanistic studies and their implications for cancer therapy. *Oncogene* **21**, 5483–5495.

Cummings, B. S., and Lash, L. H. (2000). Metabolism and toxicity of trichloroethylene and s-(1,2-dichlorovinyl)-l-cysteine in freshly isolated human proximal tubular cells. *Toxicol. Sci.* **53**, 458–466.

Cummings, B. S., Lasker, J. M., and Lash, L. H. (2000b). Expression of glutathione-dependent enzymes and cytochrome p450s in freshly isolated and primary cultures of proximal tubular cells from human kidney. *J. Pharmacol. Exp. Ther.* **293**, 677–685.

Dagtas, A. S., Edens, R. E., and Gilbert, K. M. (2009). Histone deacetylase inhibitor uses p21(Cip1) to maintain anergy in CD4+ T cells. *Int. Immunopharmacol.* **9**, 1289–1297.

di Pietro, A., Koster, R., Boersma-van Eck, W., Dam, W. A., Mulder, N. H., Gietema, J. A., de Vries, E. G., and de Jong, S. (2012). Pro- and anti-apoptotic effects of p53 in cisplatin-treated human testicular cancer are cell context-dependent. *Cell Cycle* **11**, 4552–4562.

Drummond, D. C., Noble, C. O., Kirpotin, D. B., Guo, Z., Scott, G. K., and Benz, C. C. (2005). Clinical development of histone deacetylase inhibitors as anticancer agents. *Annu. Rev. Pharmacol. Toxicol.* **45**, 495–528.

el-Deiry, W. S., Harper, J. W., O'Connor, P. M., Velculescu, V. E., Canman, C. E., Jackman, J., Pietenpol, J. A., Burrell, M., Hill, D. E., and Wang, Y. (1994). WAF1/Cip1 is induced in p53-mediated G1 arrest and apoptosis. *Cancer Res.* **54**, 1169–1174.

Faircloth, B. C., and Glenn, T. C. (2012). Not all sequence tags are created equal: Designing and validating sequence identification tags robust to indels. *PLoS One* **7**, e42543.

Fang, J. Y., Chen, Y. X., Lu, J., Lu, R., Yang, L., Zhu, H. Y., Gu, W. Q., and Lu, L. G. (2004). Epigenetic modification regulates both expression of tumor-associated genes and cell cycle progressing in human colon cancer cell lines: Colo-320 and SW1116. *Cell Res.* **14**, 217–226.

Gartel, A. L., and Radhakrishnan, S. K. (2005). Lost in transcription: p21 repression, mechanisms, and consequences. *Cancer Res.* **65**, 3980–3985.

Geneious 8.1.9. (2017). Bioinformatics Tools for Molecular Biology and NGS Analysis. New Zealand; [accessed 2019 Jan 23]. Available at: http://www.geneious.com/.

Glenn, T. C., Nilsen, R., Kieran, T. J., Finger, J. W., Pierson, T. W., Bentley, K. E., Hoffberg, S., Louha, S., Garcia-De-Leon, F. J., Portilla M. A. D. R., *et al.* (2016). Adapterama i: Universal stubs and primers for thousands of dual-indexed Illumina libraries (iTru & iNext).

Glenn, T.C., (2017). TaggiMatrix iTru. Athens (GA): BadDNA; Available at: http://baddna.uga.edu/tools-taggi.html. Accessed January 23, 2019.

Gui, C. Y., Ngo, L., Xu, W. S., Richon, V. M., and Marks, P. A. (2004). Histone deacetylase (HDAC) inhibitor activation of p21WAF1 involves changes in promoter-associated proteins, including HDAC1. *Proc. Natl. Acad. Sci. U.S.A.* **101**, 1241–1246.

Huang, J. X., Kaeslin, G., Ranall, M. V., Blaskovich, M. A., Becker, B., Butler, M. S., Little, M. H., Lash, L. H., and Cooper, M. A. (2015). Evaluation of biomarkers for *in vitro* prediction of drug-induced nephrotoxicity: Comparison of HK-2, immortalized human proximal tubule epithelial, and primary cultures of human proximal tubular cells. *Pharmacol. Res. Perspect.* **3**, e00148.

IARC (1999). Monographs on the Evaluation of Carcinogenic Risks to Humans. Lyon (France): World Health Organization; [updated 2019 Jan 15, accessed 2019 Jan 23]. Available at: http://monographs.iarc.fr/.

Illumina (2013). Bcl2fastq2 Conversion Software v2.19.1. Illumina Inc., San Diego (CA). Available at: https://support.illumina.com/downloads/bcl2fastq-conversion-software-v2-19.html. Accessed January 23, 2019.

Jiang, M., and Dong, Z. (2008). Regulation and pathological role of p53 in cisplatin nephrotoxicity. *J. Pharmacol. Exp. Ther.* **327**, 300–307.

Kawanishi, S., and Murata, M. (2006). Mechanism of DNA damage induced by bromate differs from general types of oxidative stress. *Toxicology* **221**, 172–178.

Kearse, M., Moir, R., Wilson, A., Stones-Havas, S., Cheung, M., Sturrock, S., Buxton, S., Cooper, A., Markowitz, S., Duran, C., *et al.* (2012). Geneious basic: An integrated and extendable desktop software platform for the organization and analysis of sequence data. *Bioinformatics* **28**, 1647–1649.

Kolisetty, N., Bull, R. J., Muralidhara, S., Costyn, L. J., Delker, D. A., Guo, Z., Cotruvo, J. A., Fisher, J. W., and Cummings, B. S. (2013). Association of brominated proteins and changes in protein expression in the rat kidney with subcarcinogenic to carcinogenic doses of bromate. *Toxicol. Appl. Pharmacol.* **272**, 391–398.

Kolisetty, N., Delker, D. A., Muralidhara, S., Bull, R. J., Cotruvo, J. A., Fisher, J. W., and Cummings, B. S. (2013). Changes in mRNA and protein expression in the renal cortex of male and female F344 rats treated with bromate. *Arch. Toxicol.* **87**, 1911–1925.

Krueger, F., and Andrews, S. R. (2011). Bismark: A flexible aligner and methylation caller for Bisulfite-Seq applications. *Bioinformatics* **27**, 1571–1572.

Krueger, F. (2012). Trim Galore. Cambridge (UK): [updated 2018 June 28, accessed 2019 Jan 23]. Available at: http://www.bioinformatics.babraham.ac.uk/projects/trim_galore/.

Kruger, D., Kapturska, D., Fischer, C., Daniel, R., and Wubet, T. (2012). Diversity measures in environmental sequences are highly dependent on alignment quality—Data from ITS and new LSU primers targeting basidiomycetes. *PLoS One* **7**, e32139.

Kurokawa, Y., Hayashi, Y., Maekawa, A., Takahashi, M., and Kokubo, T. (1982). Induction of renal cell tumors in F-344 rats by oral administration of potassium bromate, a food additive. *Gan* **73**, 335–338.

Kurokawa, Y., Maekawa, A., Takahashi, M., and Hayashi, Y. (1990). Toxicity and carcinogenicity of potassium bromate—a new renal carcinogen. *Environ. Health Perspect.* **87**, 309–335.

Li, L. C., and Dahiya, R. (2002). Methprimer: Designing primers for methylation PCRs. *Bioinformatics* **18**, 1427–1431.

Lin, Y. C., Lin, J. H., Chou, C. W., Chang, Y. F., Yeh, S. H., and Chen, C. C. (2008). Statins increase p21 through inhibition of histone deacetylase activity and release of promoter-associated HDAC1/2. *Cancer Res.* **68**, 2375–2383.

Masser, D. R., Berg, A. S., and Freeman, W. M. (2013). Focused, high accuracy 5-methylcytosine quantitation with base resolution by benchtop next-generation sequencing. *Epigenetics Chromatin* **6**, 33.

Meissner, A., Gnirke, A., Bell, G. W., Ramsahoye, B., Lander, E. S., and Jaenisch, R. (2005). Reduced representation bisulfite sequencing for comparative high-resolution DNA methylation analysis. *Nucleic Acids Res.* **33**, 5868–5877.

Mitani, Y., Oue, N., Hamai, Y., Aung, P. P., Matsumura, S., Nakayama, H., Kamata, N., and Yasui, W. (2005). Histone H3 acetylation is associated with reduced p21(WAF1/Cip1) expression by gastric carcinoma. *J. Pathol.* **205**, 65–73.

Moreira, P. R., Guimaraes, M. M., Guimaraes, A. L., Diniz, M. G., Gomes, C. C., Brito, J. A., and Gomez, R. S. (2009). Methylation of p16, p21, p27, RB1 and p53 genes in odontogenic keratocysts. *J. Oral Pathol. Med.* **38**, 99–103.

Nowak, G., Price, P. M., and Schnellmann, R. G. (2003). Lack of a functional p21WAF1/Cip1 gene accelerates caspase-independent apoptosis induced by cisplatin in renal cells. *Am. J. Physiol. Renal Physiol.* **285**, F440–450.

Price, P. M., Safirstein, R. L., and Megyesi, J. (2009). The cell cycle and acute kidney injury. *Kidney Int.* **76**, 604–613.

Richon, V. M., Sandhoff, T. W., Rifkind, R. A., and Marks, P. A. (2000). Histone deacetylase inhibitor selectively induces

p21WAF1 expression and gene-associated histone acetylation. *Proc. Natl. Acad. Sci. U.S.A.* **97**, 10014–10019.

Scholpa, N. E., Kolli, R. T., Moore, M., Arnold, R. D., Glenn, T. C., and Cummings, B. S. (2016). Nephrotoxicity of epigenetic inhibitors used for the treatment of cancer. *Chem. Biol. Interact.* **258**, 21–29.

Scholpa, N. E., Zhang, X., Kolli, R. T., and Cummings, B. S. (2014). Epigenetic changes in p21 expression in renal cells after exposure to bromate. *Toxicol. Sci.* **141**, 432–440.

Shin, J. Y., Kim, H. S., Park, J., Park, J. B., and Lee, J. Y. (2000). Mechanism for inactivation of the KIP family cyclin-dependent kinase inhibitor genes in gastric cancer cells. *Cancer Res.* **60**, 262–265.

Sowa, Y., Orita, T., Minamikawa, S., Nakano, K., Mizuno, T., Nomura, H., and Sakai, T. (1997). Histone deacetylase inhibitor activates the WAF1/Cip1 gene promoter through the Sp1 sites. *Biochem. Biophys. Res. Commun.* **241**, 142–150.

Teramen, H., Tsukuda, K., Tanaka, N., Ueno, T., Kubo, T., Ando, M., Soh, J., Asano, H., Pass, H. I., Toyooka, S., *et al.* (2011). Aberrant methylation of p21 gene in lung cancer and malignant pleural mesothelioma. *Acta Med. Okayama* **65**, 179–184.

Todd, J. H., McMartin, K. E., and Sens, D. A. (1996). Enzymatic isolation and serum-free culture of human renal cells: Retaining properties of proximal tubule cells. *Methods Mol. Med.* **2**, 431–435.

US-EPA. (1998a). Stage 1 and stage 2 disinfectants and disinfection byproducts rules. Washington, DC: United States Environmental Protection Agency; [updated 2018 Dec 21; accessed 2019 Jan 23]. Available at: https://www.epa.gov/dwreginfo/stage-1-and-stage-2-disinfectants-and-disinfection-byproducts-rules

US-EPA. (1998b). National primary drinking water regulations: Disinfectants and disinfection byproducts; final rule. Washington, DC. United States Environmental Protection Agency; [accessed 2019 Jan 24]. Available at: https://nepis.epa.gov/Exe/ZyPDF.cgi/200023ZG.PDF?Dockey=200023ZG.PDF

US-EPA. (2012). Integrated risk information system. Washington, DC: United States Environmental Protection Agency; [updated 2018 Dec 19; accessed 2019 Jan 23]. Available at: https://www.epa.gov/iris.

Vanhaecke, T., Papeleu, P., Elaut, G., and Rogiers, V. (2004). Trichostatin A-like hydroxamate histone deacetylase inhibitors as therapeutic agents: Toxicological point of view. *Curr. Med. Chem.* **11**, 1629–1643.

Varley, K. E., Gertz, J., Bowling, K. M., Parker, S. L., Reddy, T. E., Pauli-Behn, F., Cross, M. K., Williams, B. A., Stamatoyannopoulos, J. A., Crawford, G. E., *et al.* (2013). Dynamic DNA methylation across diverse human cell lines and tissues. *Genome Res.* **23**, 555–567.

VirtualBox VM. (2007). Weinstadt (Germany): Oracle; [updated 2019 Jan 15, accessed 2019 Jan 23]. Available at: https://www.virtualbox.org/.

Wolf, D. C., Crosby, L. M., George, M. H., Kilburn, S. R., Moore, T. M., Miller, R. T., and DeAngelo, A. B. (1998). Time- and dose-dependent development of potassium bromate-induced tumors in male Fischer 344 rats. *Toxicol. Pathol.* **26**, 724–729.

Ying, J., Srivastava, G., Gao, Z., Zhang, X., Murray, P., Ambinder, R., and Tao, Q. (2004). Promoter hypermethylation of the cyclin-dependent kinase inhibitor (CDKI) gene p21WAF1/Cip1/SDI1 is rare in various lymphomas and carcinomas. *Blood* **103**, 743–746.

Yoon, M. K., Mitrea, D. M., Ou, L., and Kriwacki, R. W. (2012). Cell cycle regulation by the intrinsically disordered proteins p21 and p27. *Biochem. Soc. Trans.* **40**, 981–988.

Yuan, H., Reddy, M. A., Sun, G., Lanting, L., Wang, M., Kato, M., and Natarajan, R. (2013). Involvement of p300/CBP and epigenetic histone acetylation in TGF-beta1-mediated gene transcription in mesangial cells. *Am. J. Physiol. Renal Physiol.* **304**, F601–613.

Zhang, X., Bull, R. J., Fisher, J., Cotruvo, J. A., and Cummings, B. S. (2011). The synergistic effect of sodium chlorite and bromochloroacetic acid on BrO3(−)-induced renal cell death. *Toxicology* **289**, 151–159.

Zhang, X., De Silva, D., Sun, B., Fisher, J., Bull, R. J., Cotruvo, J. A., and Cummings, B. S. (2010). Cellular and molecular mechanisms of bromate-induced cytotoxicity in human and rat kidney cells. *Toxicology* **269**, 13–23.